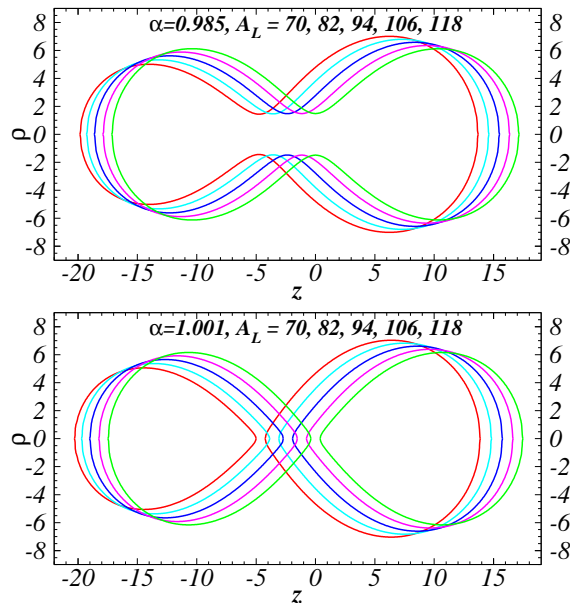

Dynamical Scission Model: Current Density and Angular Distribution of Scission Neutrons

N. Carjan^{1,2}, M. Rizea²,

(1) CENBG, CNRS/IN2P3 - Université Bordeaux 1, France

**(2) "Horia Hulubei" National Institute of Physics and
Nuclear Engineering, Bucharest, Romania**

Modeling a diabatic transition at scission (neck rupture)



A fast transition at scission produces the excitation of all neutrons that are present in the surface region. For few of them this excitation exceeds their binding and they are released.

The mass asymmetry was introduced in: N.Carjan, M.Rizea, Phys.Rev.C82(2010)014617 (still in the sudden approx)

Going beyond the sudden approximation

A time-dependent approach to the fast transition at scission:

$\{\alpha^i\} \rightarrow \{\alpha^f\}$; *i and f meaning just-before and immediately-after.*

Features of this **scission model**:

- 1) **dynamical**: it takes into account the duration ΔT of the neck rupture and its integration in the fragments
- 2) **microscopic**: it calculates the time evolution of each occupied neutron state
- 3) **fully quantum mechanical**: it uses the two-dimensional time-dependent Schrödinger equation (TDSE2D) with time-dependent potential (TDP).

Most previous models were statical, statistical and semiclassical: Fong (1963), Wilkins et al. (1976), etc.

The picture behind the present model was first proposed by Fuller (Wheeler) in 1962 and illustrated by a "volcano erupting" in the middle of a Fermi sea.

Plan

- **Excitation energy at scission** can be generated during:
 - 1) saddle to just-before scission descent (relatively slow)
 - 2) neck rupture (extremely fast). $\langle \Delta V / \Delta T \rangle$Focus on single-particle excitations (and their partition between the fission fragments) due to the coupling between the collective and intrinsic degrees of freedom.
- **Unbound neutrons at scission**: multiplicities, probability density and current density.
- Angular distribution with respect to the fission axis
- Summary and conclusions.
- Last publication:
M. Rizea, N. Carjan, Nucl. Phys. A 909 (2013) 50

Dynamical scission model: formalism

It is a generalization of the sudden approximation. Let $|\Psi^i\rangle$, $|\Psi^f\rangle$ be the eigenfunctions corresponding to the just-before-scission and immediately-after-scission configurations respectively. The propagated wave functions $|\Psi^i(t)\rangle$ are wave packets that have also some positive-energy components. The probability amplitude that a neutron occupying the state $|\Psi^i\rangle$ before scission populates a state $|\Psi^f\rangle$ after scission is

$$a_{if} = \langle \Psi^i(T) | \Psi^f \rangle = 2\pi \int \int (g_1^i(T)g_1^f + g_2^i(T)g_2^f) d\rho dz.$$

The result strongly depends on the duration T of the scission process.

Excitation energy of the fission fragments

The total occupation probability of a given final eigenstate is:

$$V_f^2 = \sum_{bound} v_i^2 |a_{if}|^2$$

where v_i^2 is the ground-state occupation probability of a given initial eigenstate. Since V_f^2 is different from v_f^2 (the ground-state value), the fragments are left in an excited state. The corresponding **excitation energy at scission** is:

$$E_{sc}^* = 2 \sum_{bound\ states} (V_f^2 - v_f^2) e_f.$$

The factor of 2 is due to the spin degeneracy.

Neutrons emitted at scission

One can also calculate the multiplicity of the neutrons released during scission:

$$\nu_{sc} = 2 \sum_{bound} v_i^2 \left(\sum_{unbound} |a_{if}|^2 \right).$$

A quantity that can clarify the emission mechanism of the scission neutrons is the probability density i.e., the spatial distribution of the emission points at $t=T$

$$S_{em}(\rho, z) = 2 * \sum_{bound} v_i^2 |\Psi_{em}^i(\rho, z, T)|^2,$$

where

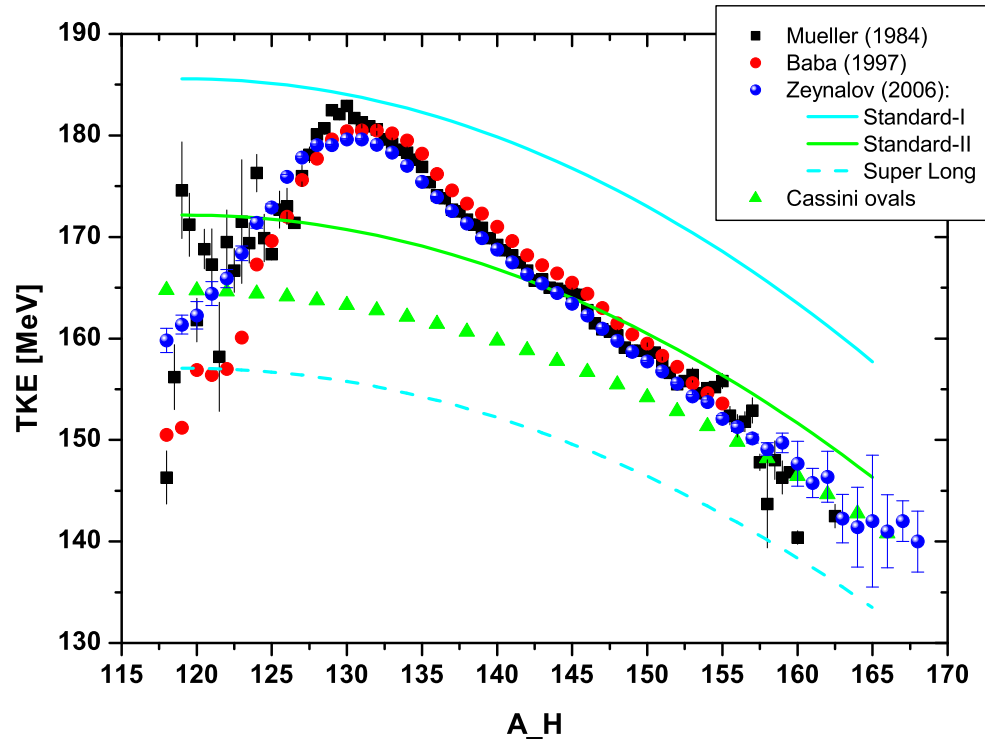
$$|\Psi_{em}^i\rangle = |\Psi^i(T)\rangle - \sum_{\text{bound states}} a_{if} |\Psi^f\rangle$$

is the part of the wave packet that is emitted.
Similarly, the current density

$$\bar{D}_{em}(\rho, z) = \frac{i\hbar}{\mu} \sum_i v_i^2 (f^i \bar{\nabla} f^{i*} - f^{i*} \bar{\nabla} f^i), \quad (1)$$

with $f^i = |\Psi_{em}^i\rangle$, provides **the distribution of the average directions of motion** of the unbound neutrons at $t=T$.
These two quantities influence the amount of neutrons that are reabsorbed, scattered or left unaffected by the fragments and finally determine their angular distribution.

Total kinetic energy of the fission fragments



8 MeV kinetic energy at scission explains the data. Our LDM estimate for the energy difference between the saddle point and the just-before-scission point (when the neck starts to break) is 11 MeV.

Pre- and post- scission configurations

We study the transition from the moment the neck starts to break to the moment the neck stubs are integrated in the fragments.

These just-before and immediately after scission configurations are defined by Cassini ovals with only two parameters ($\alpha=0.985, \alpha_1$) and ($\alpha=1.001, \alpha_1$) respectively; α_1 defines the mass asymmetry.

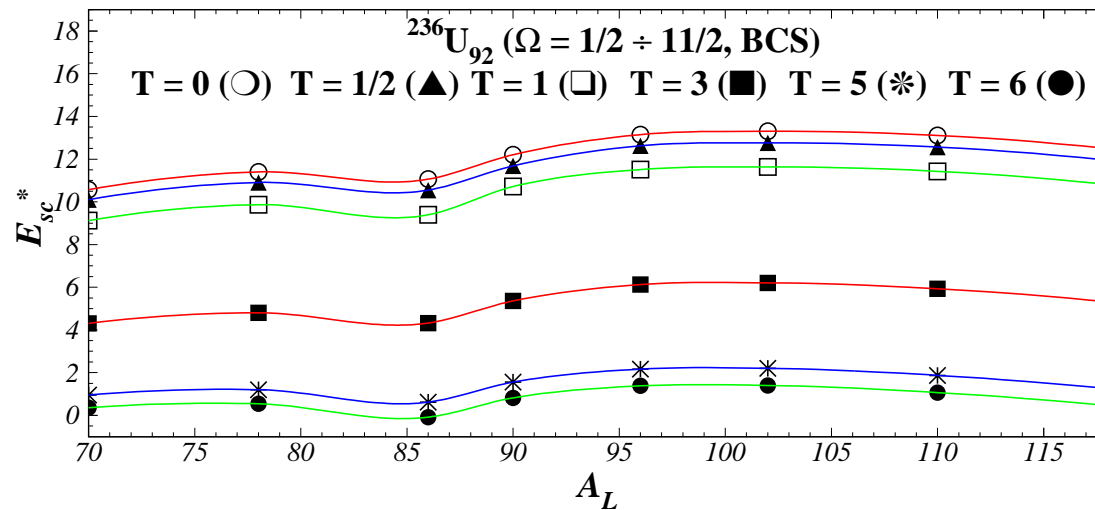
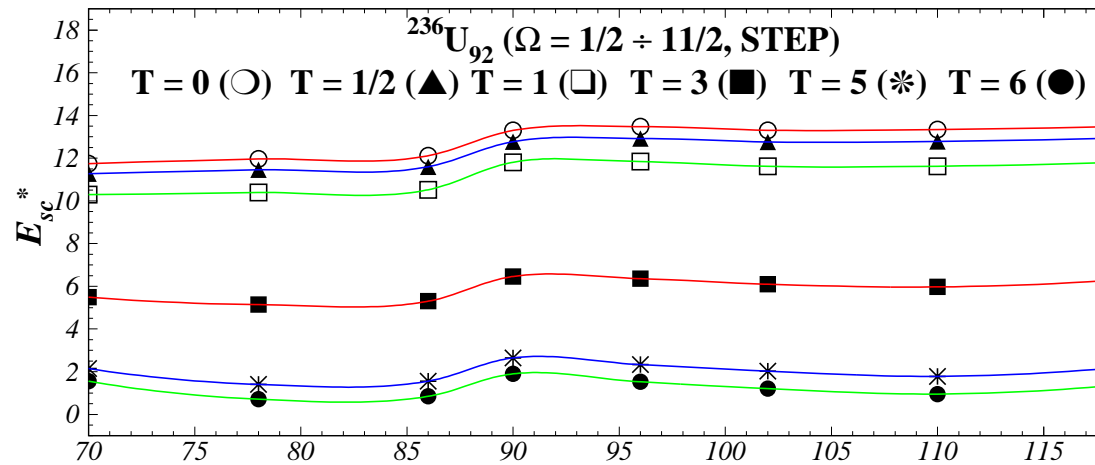
For the choice of the first configuration we have good arguments.

The choice of the second configuration is quite arbitrary. Comparison with experimental data should be used to improve it.

The exact duration ΔT of this transition is also unknown. Values from 1×10^{-22} to 6×10^{-22} sec are used.

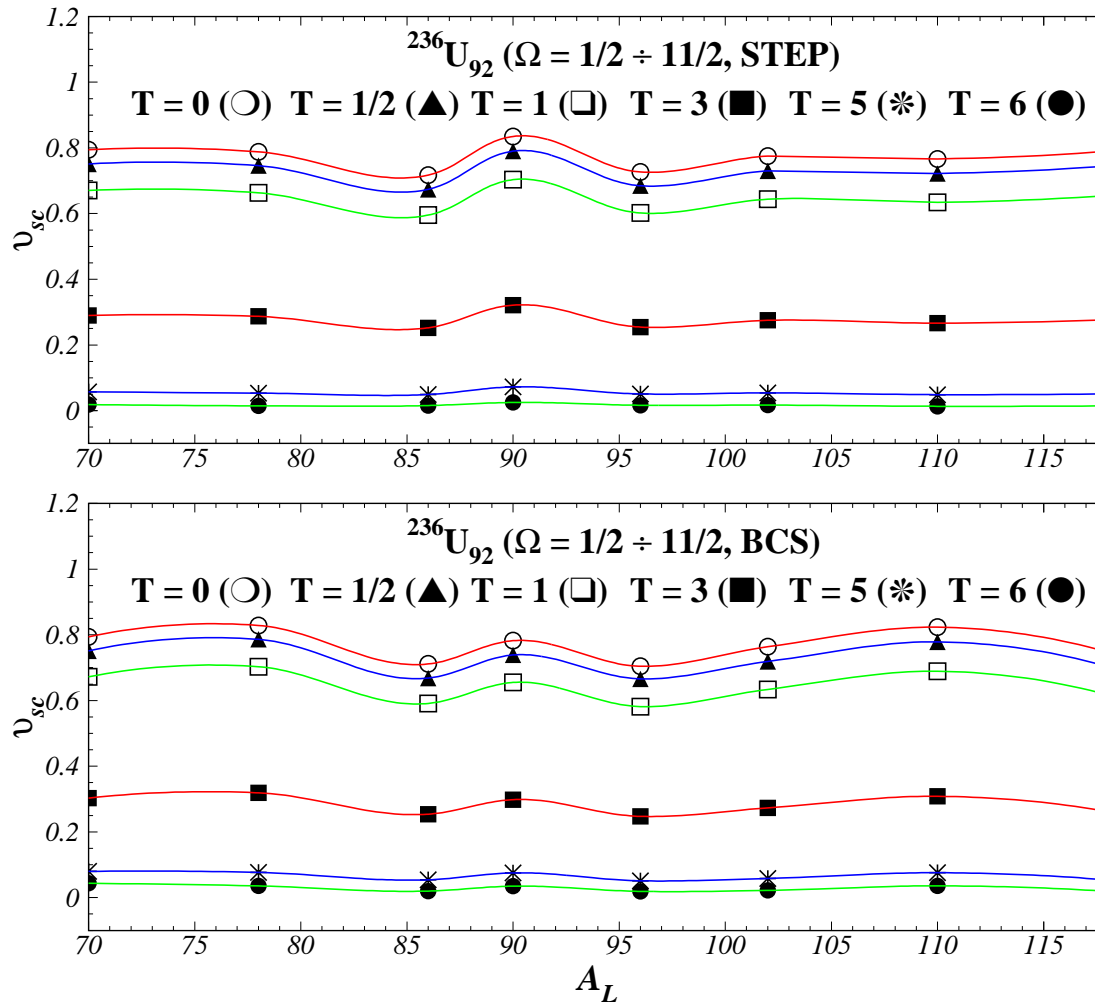
Excitation energy as a function of transition time T

for $T=10^{-22}$ sec the values are 20% below the sudden limit



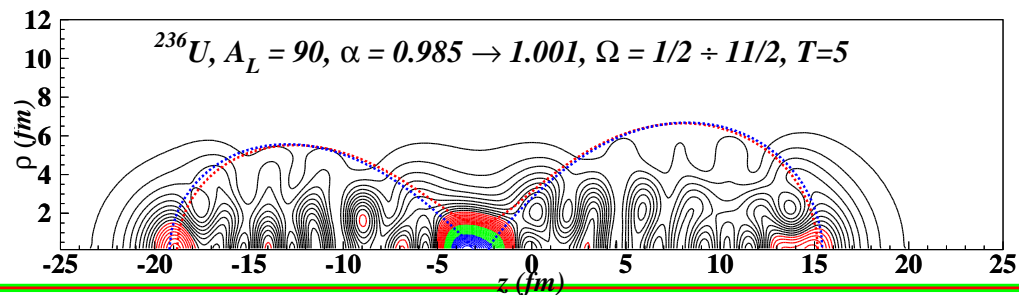
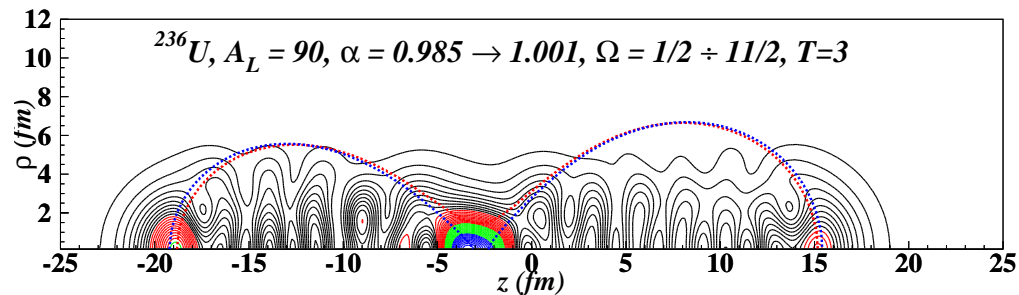
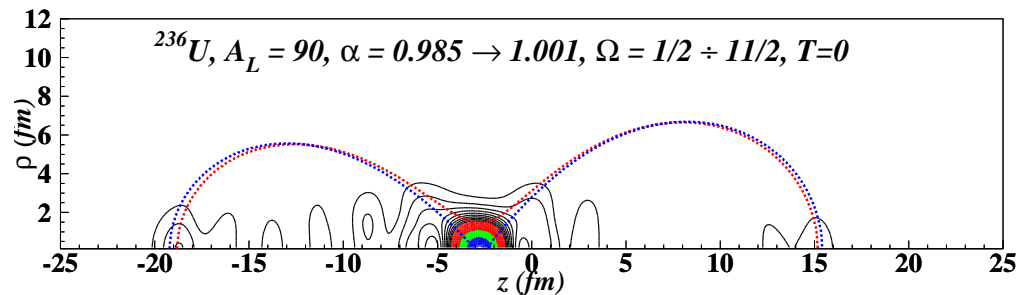
Neutron multiplicity as a function of transition time

a smooth occupation-probability function produces little change



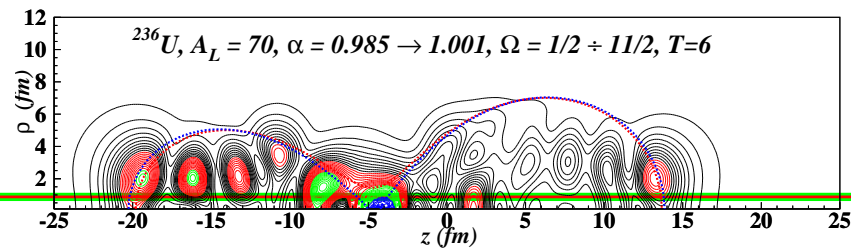
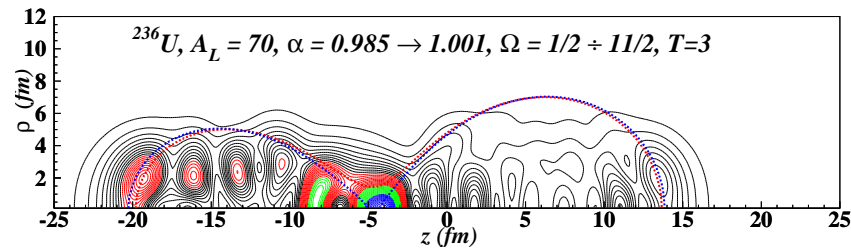
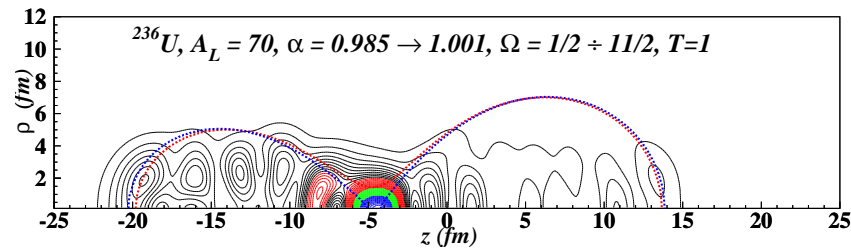
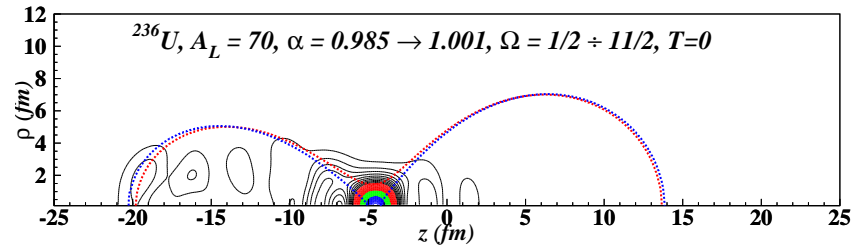
Emission points ($A_L=90$; all Ω ; $T=0,3,5 \times 10^{-22}$ sec)

with increasing T the emission points slightly migrate from the H to the L fragment and from the inter-fragment to the inside-fragment regions



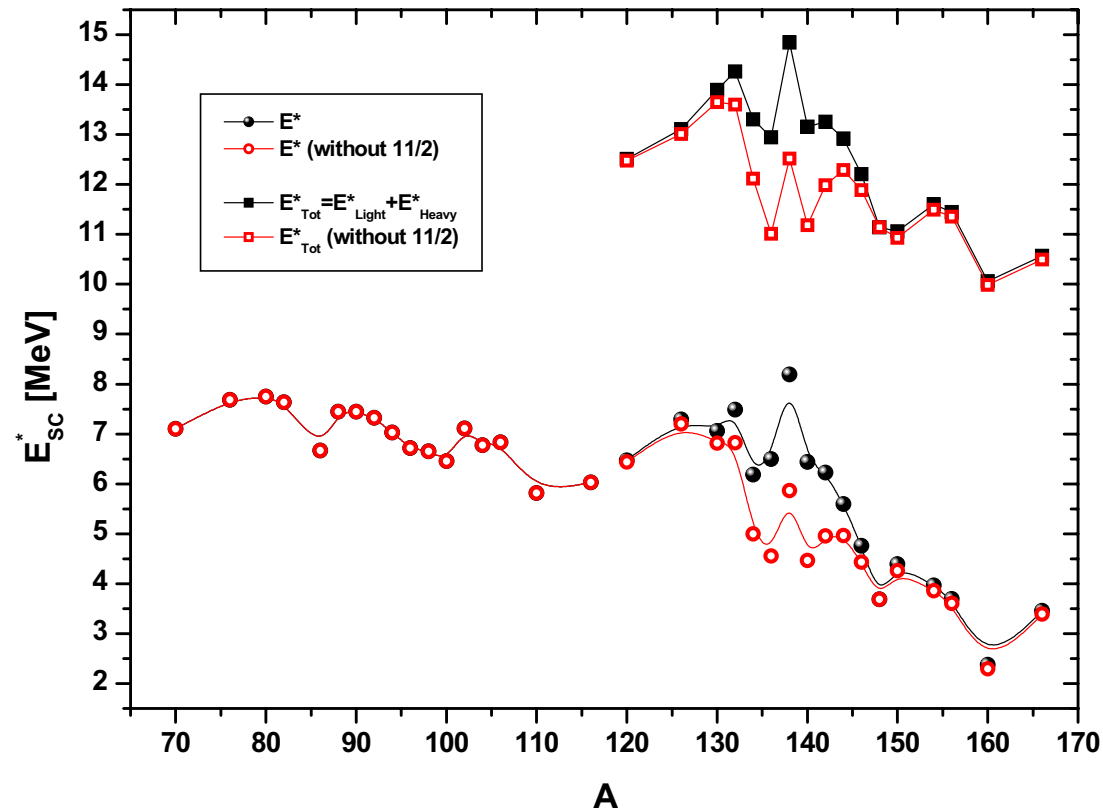
Emission points ($A_L=70$; all Ω ; $T=0,1,3,6 \times 10^{-22}$ sec)

for this asymmetry the migration from L to H is even more pronounced



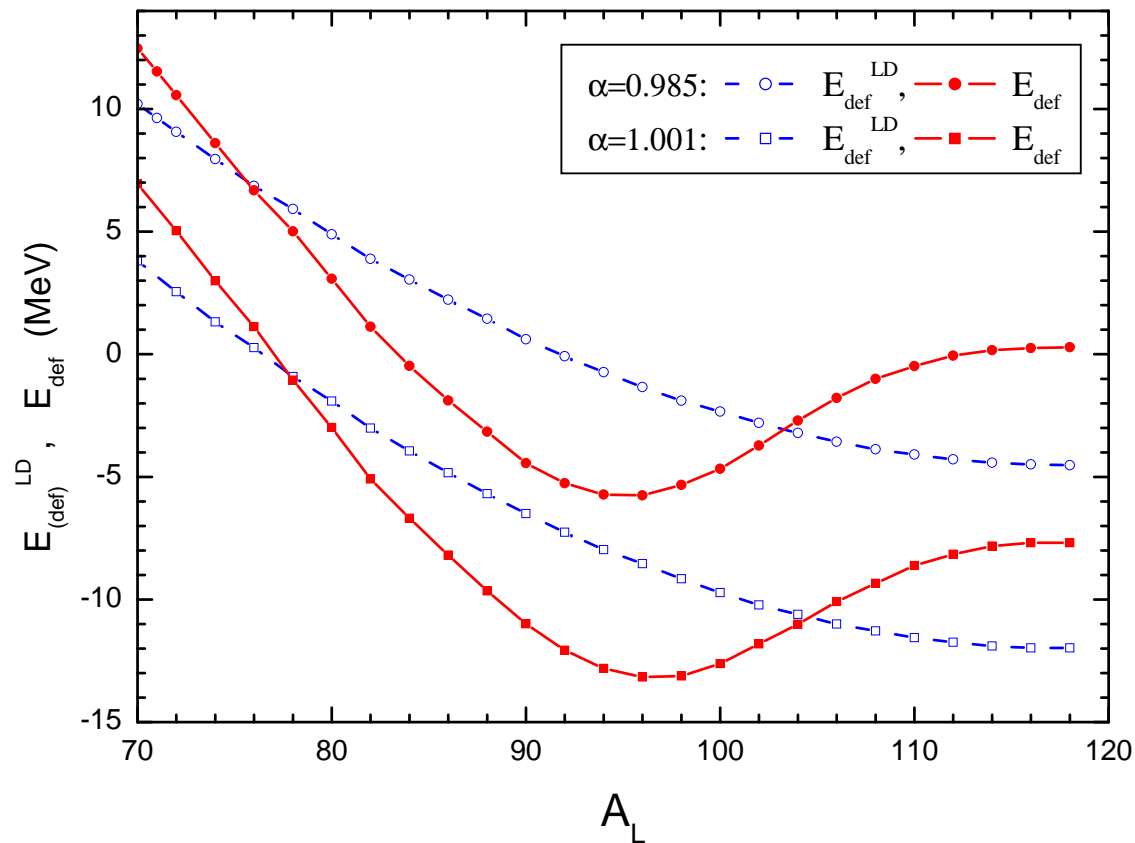
Excitation energy immediately after scission

N.Carjan,F.-J.Hambsch,M.Rizea,O.Serot, PR C85 (2012)



created *only* during the sudden neck rupture; it decreases with mass asymmetry

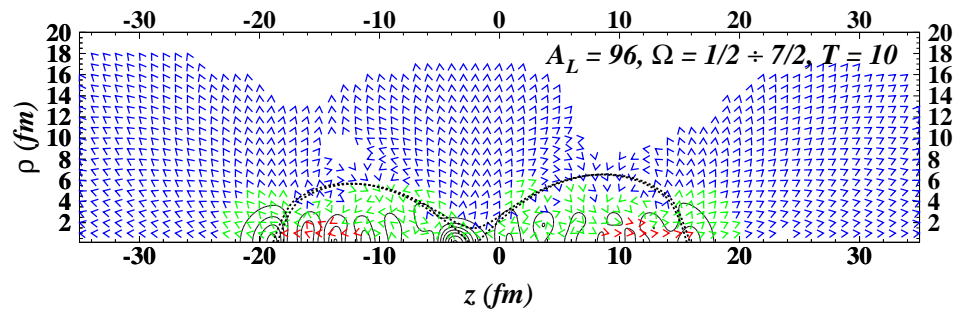
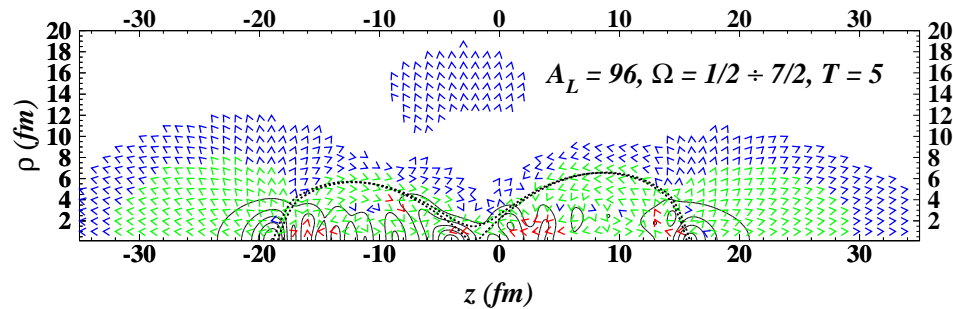
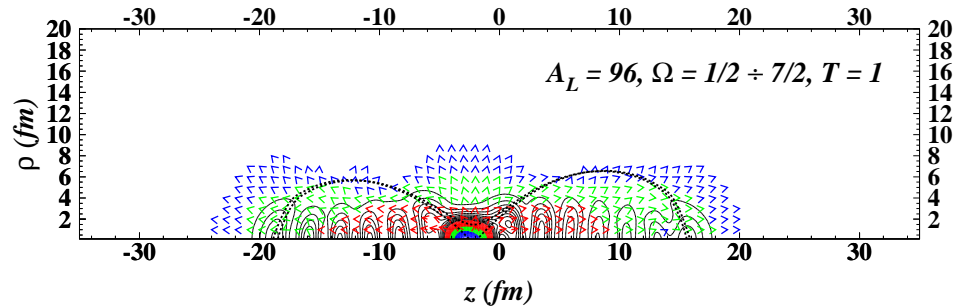
Deformation energy before and after scission



the available energy ΔE_{def} is also decreasing with increasing mass asymmetry

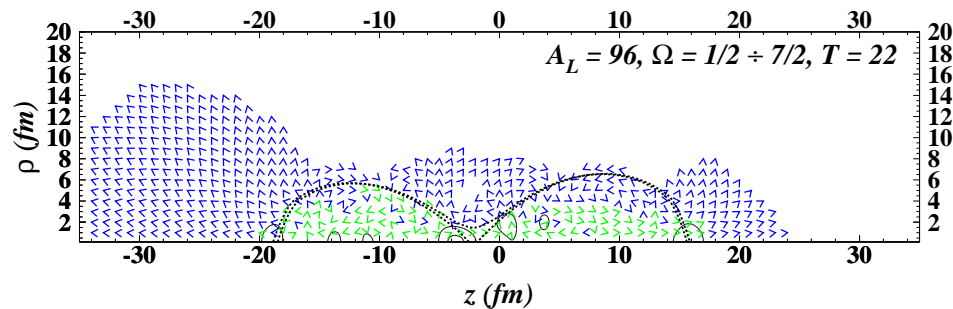
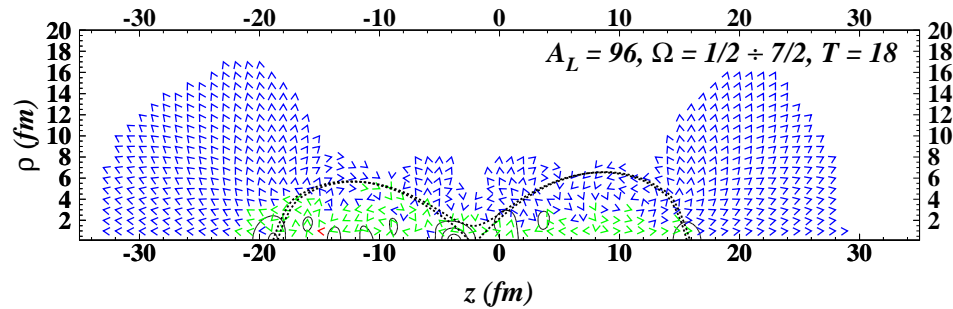
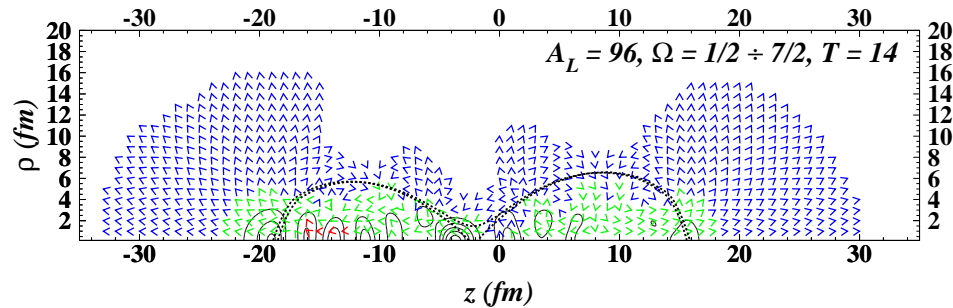
Emission directions ($A_L=96$; all Ω ; $T=1,5,10 \times 10^{-22}$ sec)

correlation between S_{em} and D_{em} ; pulsed emission perpendicular



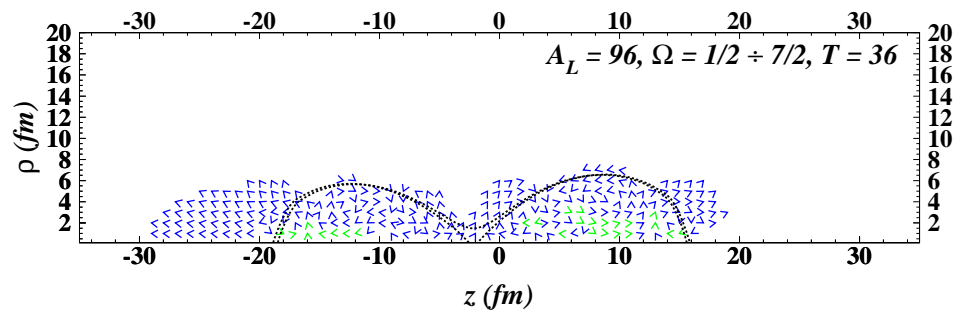
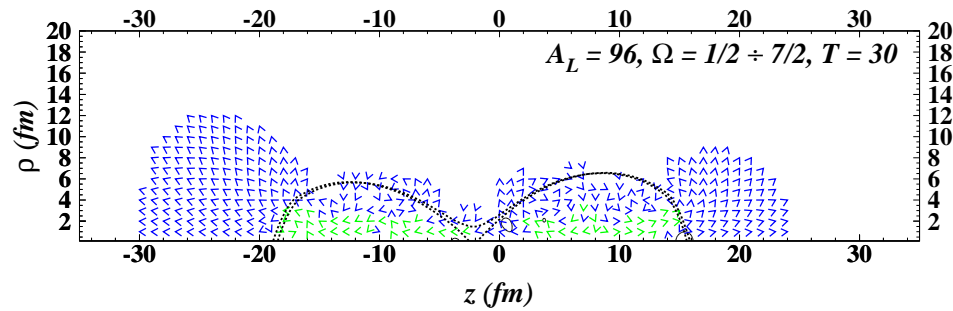
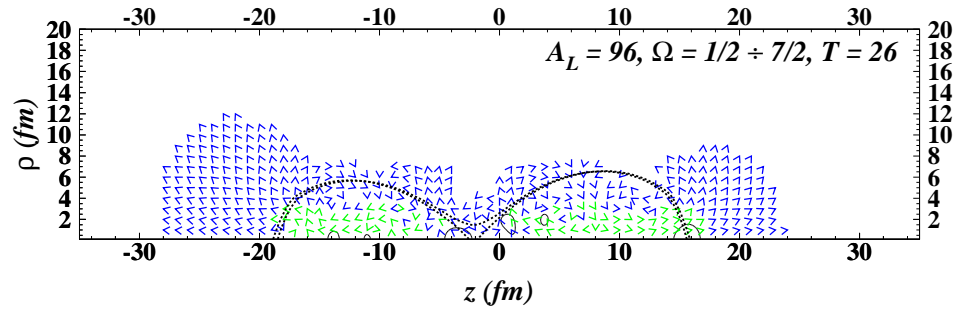
Emission directions ($A_L=96$; all Ω ; $T=14,18,22 \times 10^{-22}$ sec)

emission along the fission axis; the light-fragment is more productive



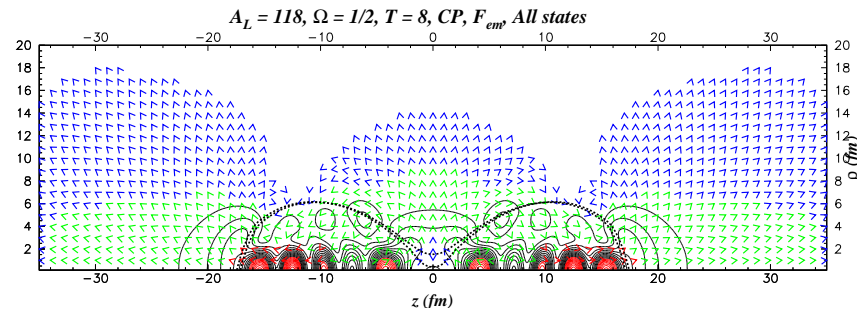
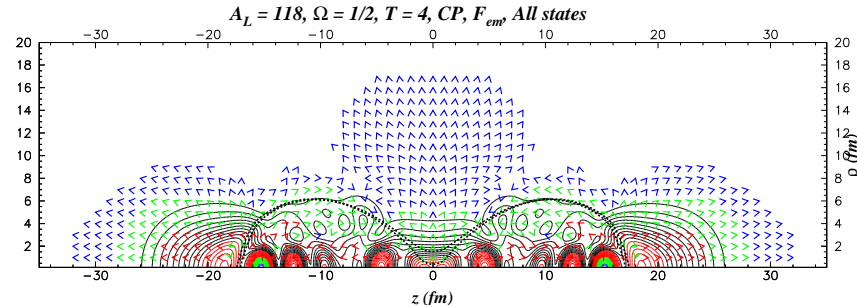
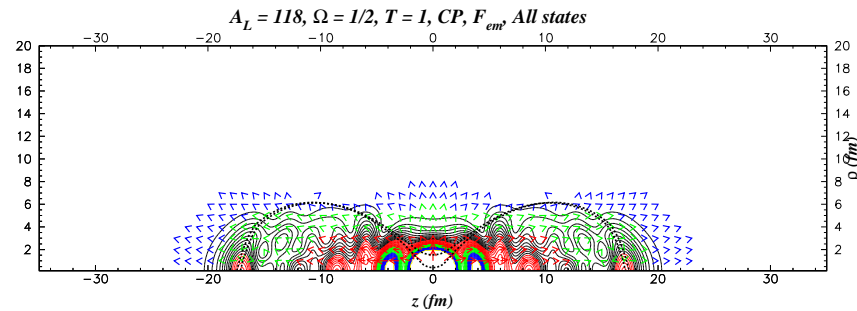
Emission directions ($A_L=96$; all Ω ; $T=26,30,36 \times 10^{-22}$ sec)

emission is slowed down; neutron transfer & reflections



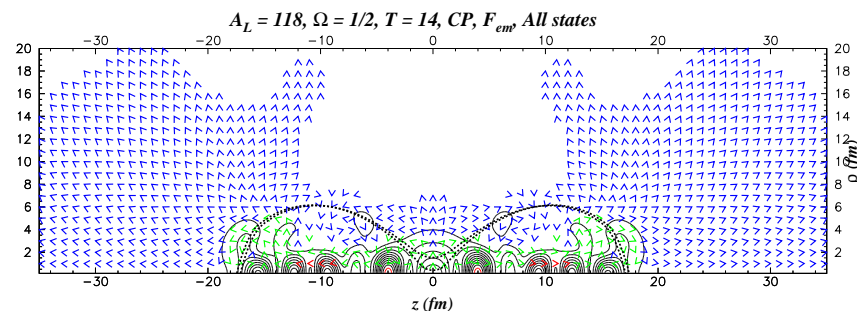
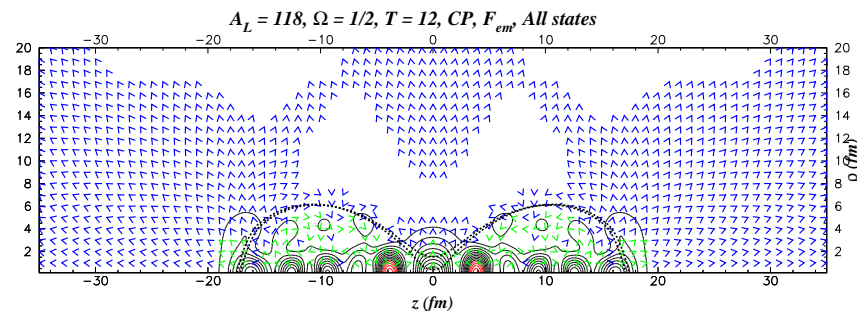
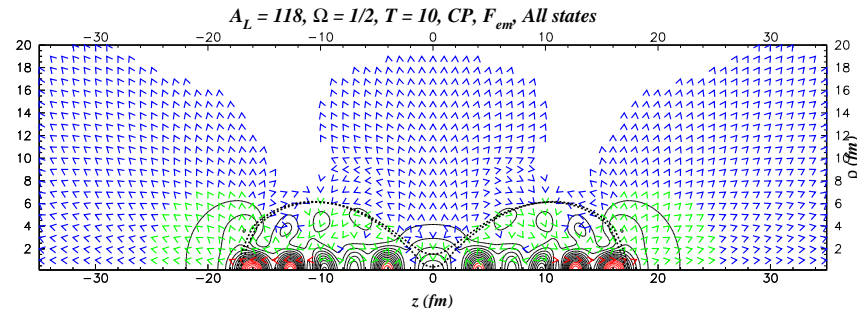
Emission directions ($A_L=118; \Omega=1/2; T=1,4,8 \times 10^{-22}$ sec)

for symmetric fission the central peak of S_{em} vanishes quickly
(for $A_L=96$ it was moving into the light fragment)



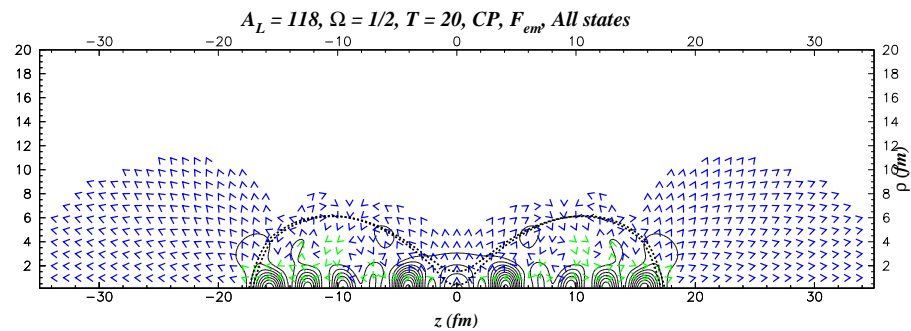
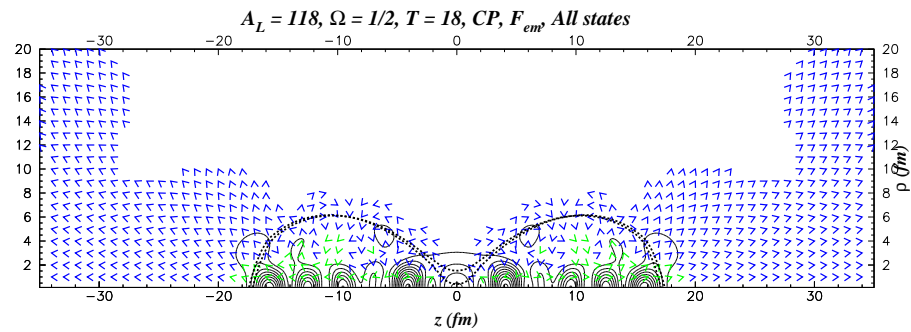
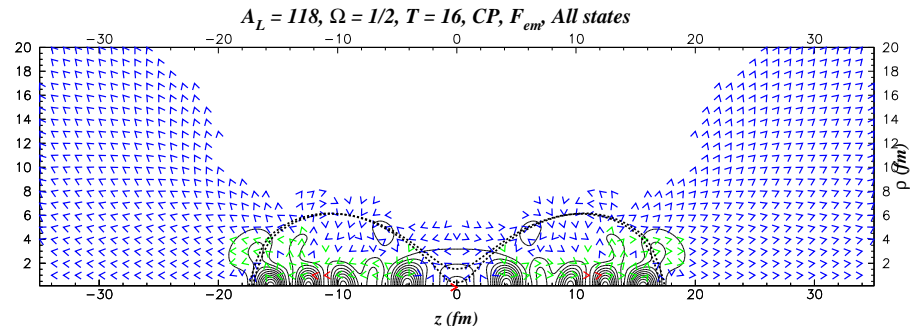
Emission directions ($A_L=118; \Omega=1/2; T=10,12,14 \times 10^{-22}$ sec)

pulsed emission perpendicular to the fission axis; polar and equatorial components seem to be comparable in intensity up to $T=10^{-21}$ sec



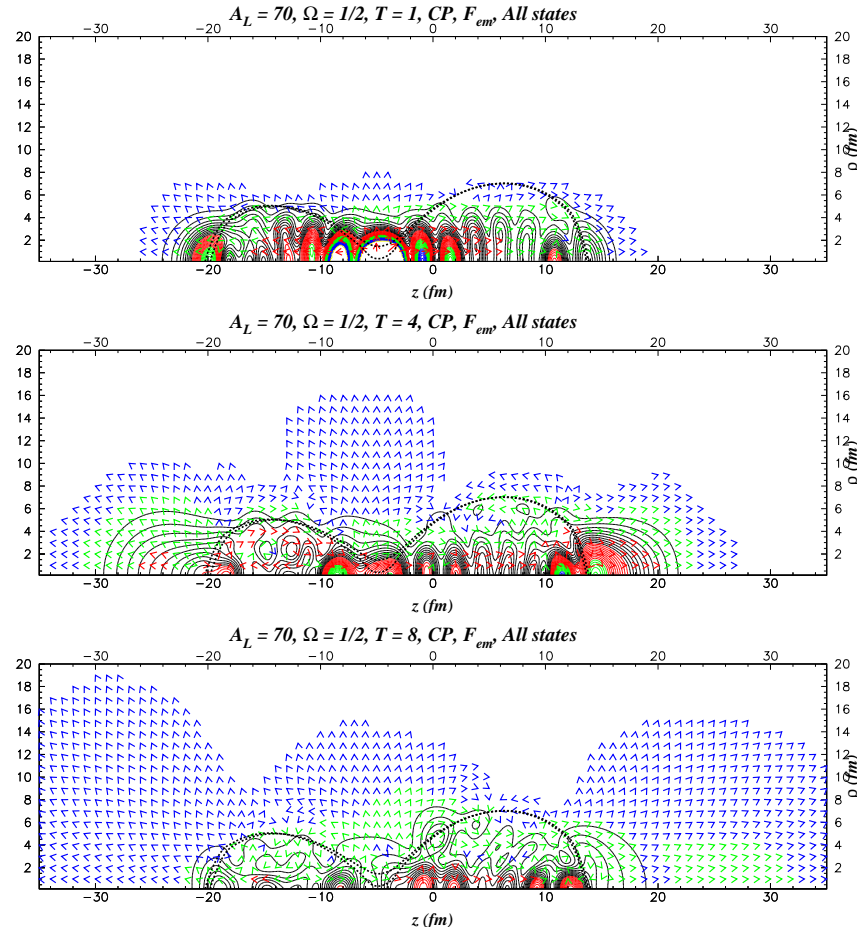
Emission directions ($A_L=118; \Omega=1/2; T=16,18,20 \times 10^{-22}$ sec)

only polar emission after 10^{-21} sec



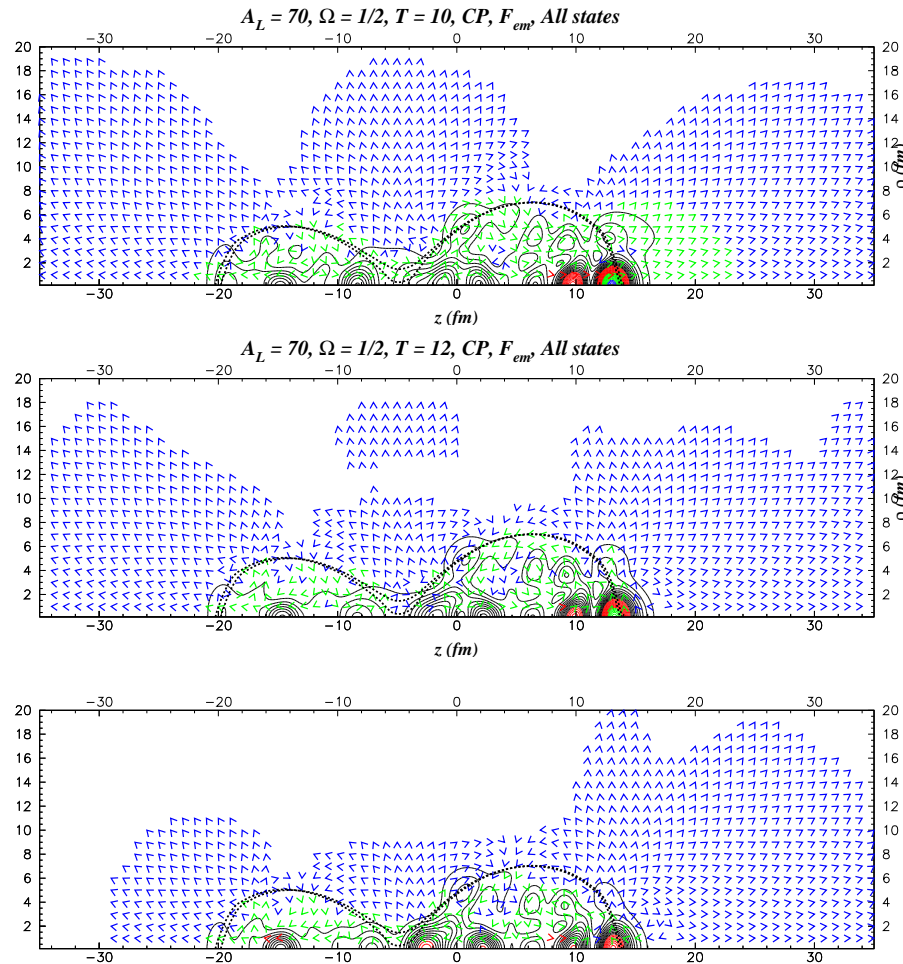
Emission directions ($A_L=70; \Omega=1/2; T=1,4,8 \times 10^{-22}$ sec)

for very asymmetric fission and at short times the emission is predominantly from the light fragment



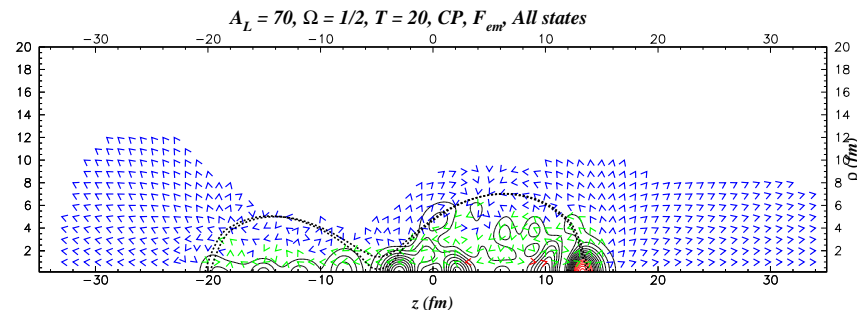
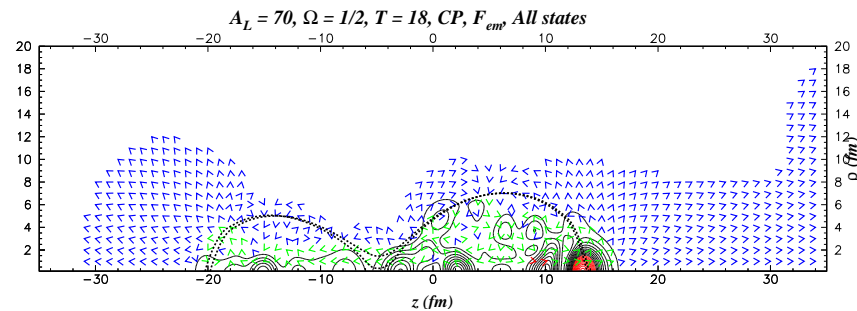
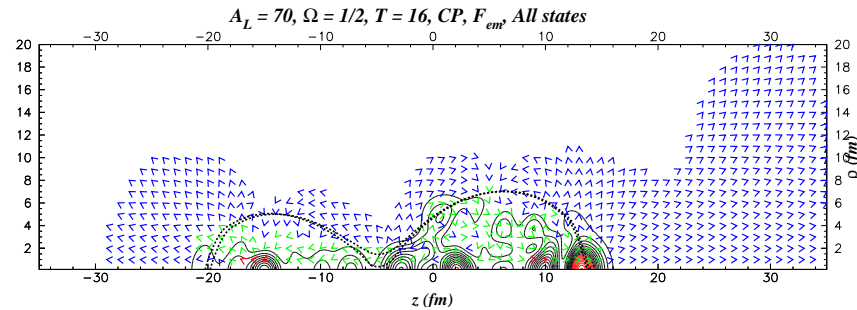
Emission directions ($A_L=70$; $\Omega=1/2$; $T=10,12,14 \times 10^{-22}$ sec)

at intermediate times the heavy fragment is picking up



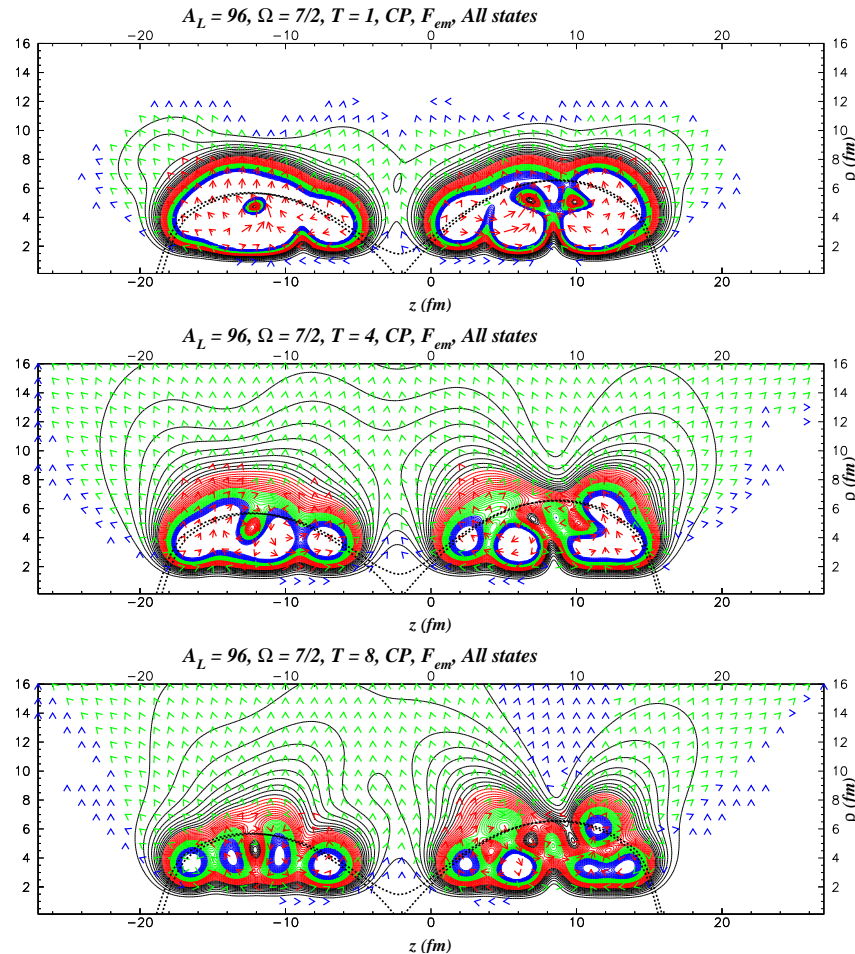
Emission directions ($A_L=70$; $\Omega=1/2$; $T=16,18,20 \times 10^{-22}$ sec)

at longer times the emission is predominantly from the heavy fragment; the light fragment has emitted all his unbound neutrons



Emission directions ($A_L=96$; $\Omega=7/2$; $T=1,4,8 \times 10^{-22}$ sec)

for high Ω values the angular distribution may have more than two peaks that are neither along nor perpendicular to the fission axis.



Angular distribution - computational procedure

The core of the **dynamical scission model** is the calculation of the time evolution of the neutron states in a nucleus that undergoes scission using the **TDSE**: [N. Carjan, M. Rizea, Int. J. Mod. Phys. E21 \(2012\) 0031125](#)

To estimate the angular distribution with respect to the fission axis of the neutrons emitted during scission we separate this calculation in two stages:

1) The **scission process** itself, i.e., the neck rupture and its absorption by the fragments. The nuclear configurations involved are defined by a set of deformations $\{\alpha_i\}$ (when the neck starts to break) and $\{\alpha_f\}$ (when the neck stubs are completely absorbed by the fragments). The duration of this stage is relatively short (e.g. $T = 10^{-22}$ sec) and the potential in which the neutrons move changes rapidly.

Angular distribution - procedure

2) The **detachment** from the fragments of the fraction of the **neutrons that are left unbound** at the end of the previous stage. Since their motion is much faster than that of the just separated fragments, one can, in a first approximation, freeze the fragments at the configuration $\{\alpha_f\}$. Hence the potential in which the neutrons move is kept constant during this stage. We follow the motion of the wave packet that describes the unbound neutrons for as long as we can (4×10^{-21} sec) and calculate the current density at each time step. To obtain the angular distribution one separates the tangential from the radial components of the current along the surface of a large sphere and integrate in time.

Angular distribution - formula

- **The number of neutrons** that leave a sphere of radius R (around the fissioning nucleus) in a solid angle $d\Omega$ and in a time interval dt is:

$$d\nu_{sc}^{em} = \bar{J}_{em}(R, \theta, t) \bar{n}(R, \theta, t) R^2 dt d\Omega.$$

- **The angular distribution** is given by the integral with respect to t of the above quantity. The upper limit should in principle be ∞ . In practice we can reach only a finite value t_{max} .

- **The total number of emitted neutrons** ν_{sc}^{em} at t_{max} is obtained by a further integration with respect to θ ($d\Omega = \sin\theta d\theta$).

A factor of 4π also appears due to the integration over the angle ϕ and to the spin degeneracy.

Application to ^{236}U

We estimated the angular distribution of the scission neutrons in the case of ^{236}U at different mass asymmetries defined by $A_L = 70, 96$ and 118 . The numerical domain is: $\rho \in [\Delta\rho, 35]$, $z \in [-35, 35]$, while $\Delta\rho = \Delta z = 0.125$ fm. The number of grid points ≈ 157000 . The time step $\Delta t = 1/256 \times 10^{-22}$ sec.

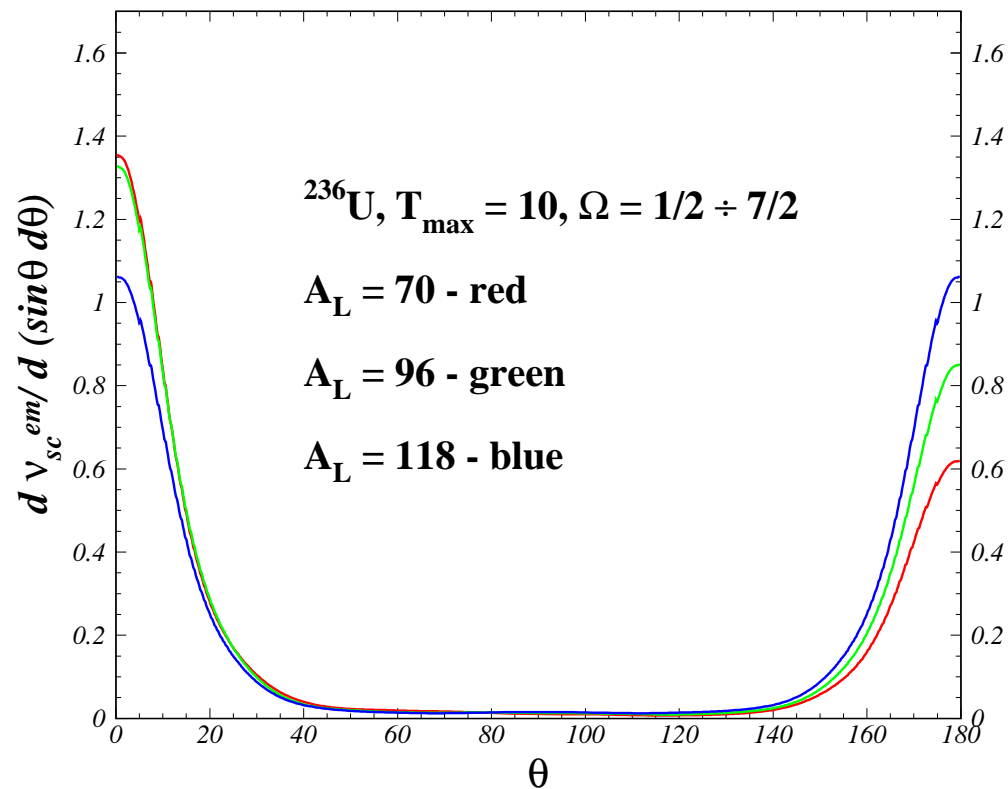
The radius of the sphere used to calculate the angular distribution is: $R = 30$ fm. Limited results are obtained also for $R = 40$ fm

$t_{max} = 4 \times 10^{-21}$ sec. At this time 75% of the neutrons left the sphere.

We consider $\Omega = 1/2, 3/2, 5/2, 7/2$ so that almost all initial states that are initially bound were taken into account.

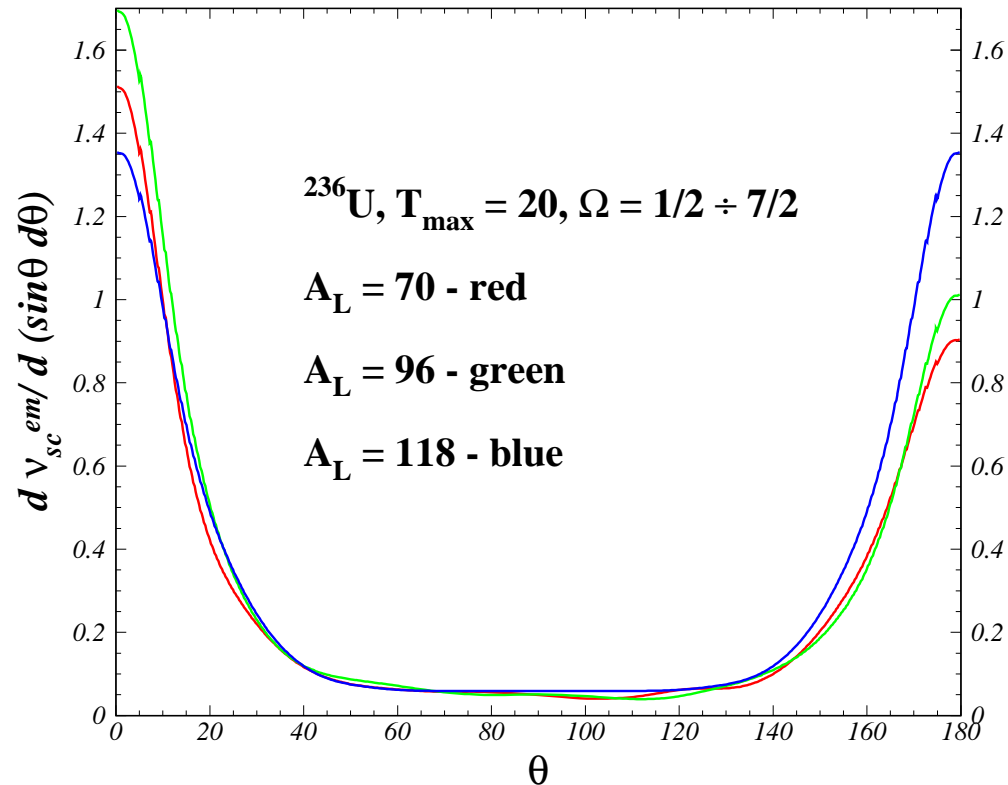
Angular distribution at $T = 10 \times 10^{-22} \text{sec}$

ν_L/ν_H depends on mass ratio A_L/A_H ; the width is slightly larger on the H-fragment side.



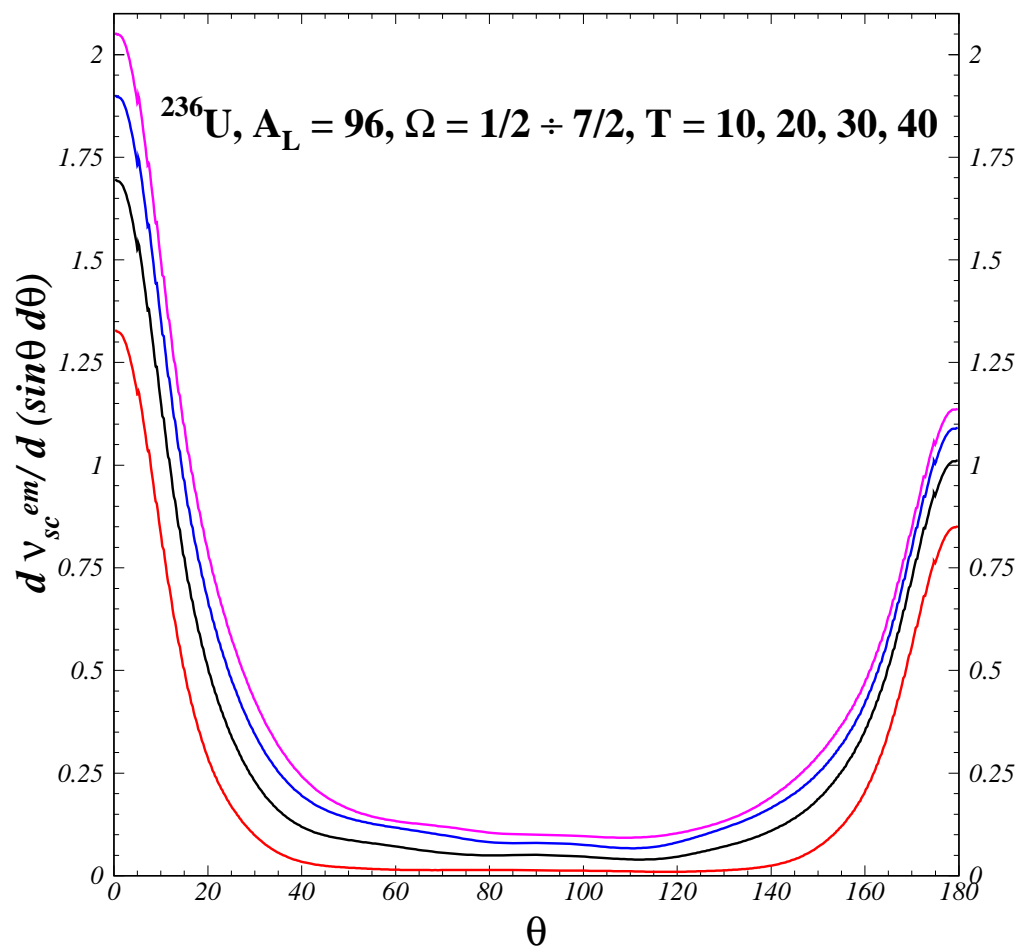
Angular distribution at $T = 20 \times 10^{-22} \text{ sec}$

ν_L/ν_H changes in time.



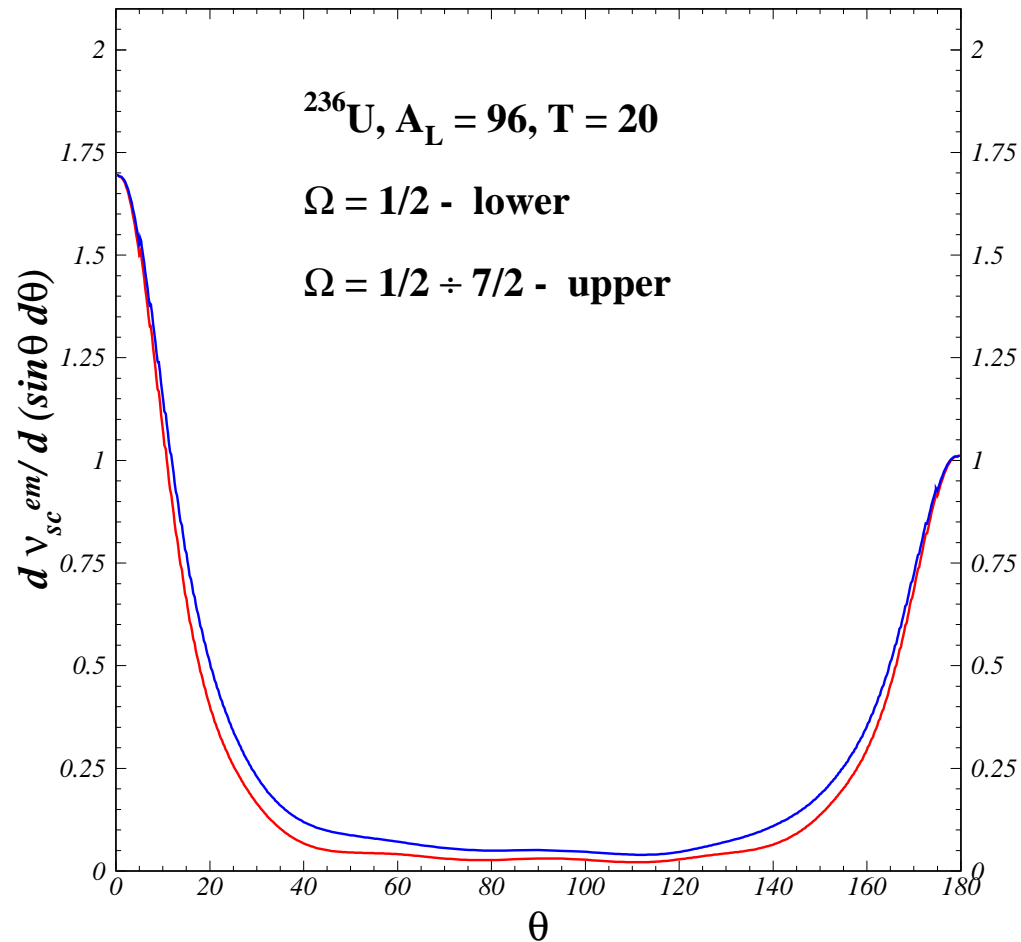
The time evolution of the ang distr for $A_L = 96$ at $R=30$ fm

L and H widths increase with increasing time T



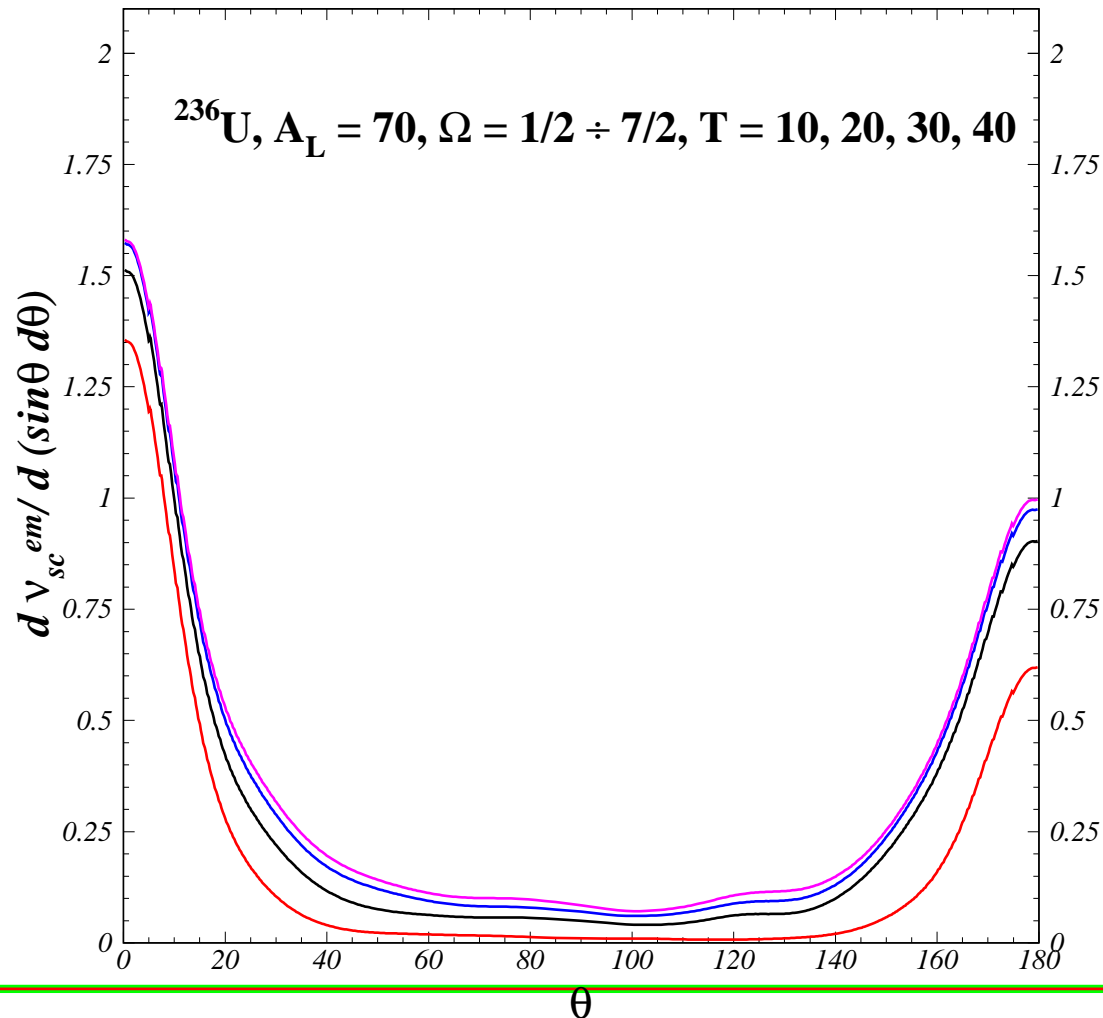
Contribution of $\Omega=1/2$ to the angular distribution

around 0° and 180° there are only neutrons with $\Omega = 1/2$



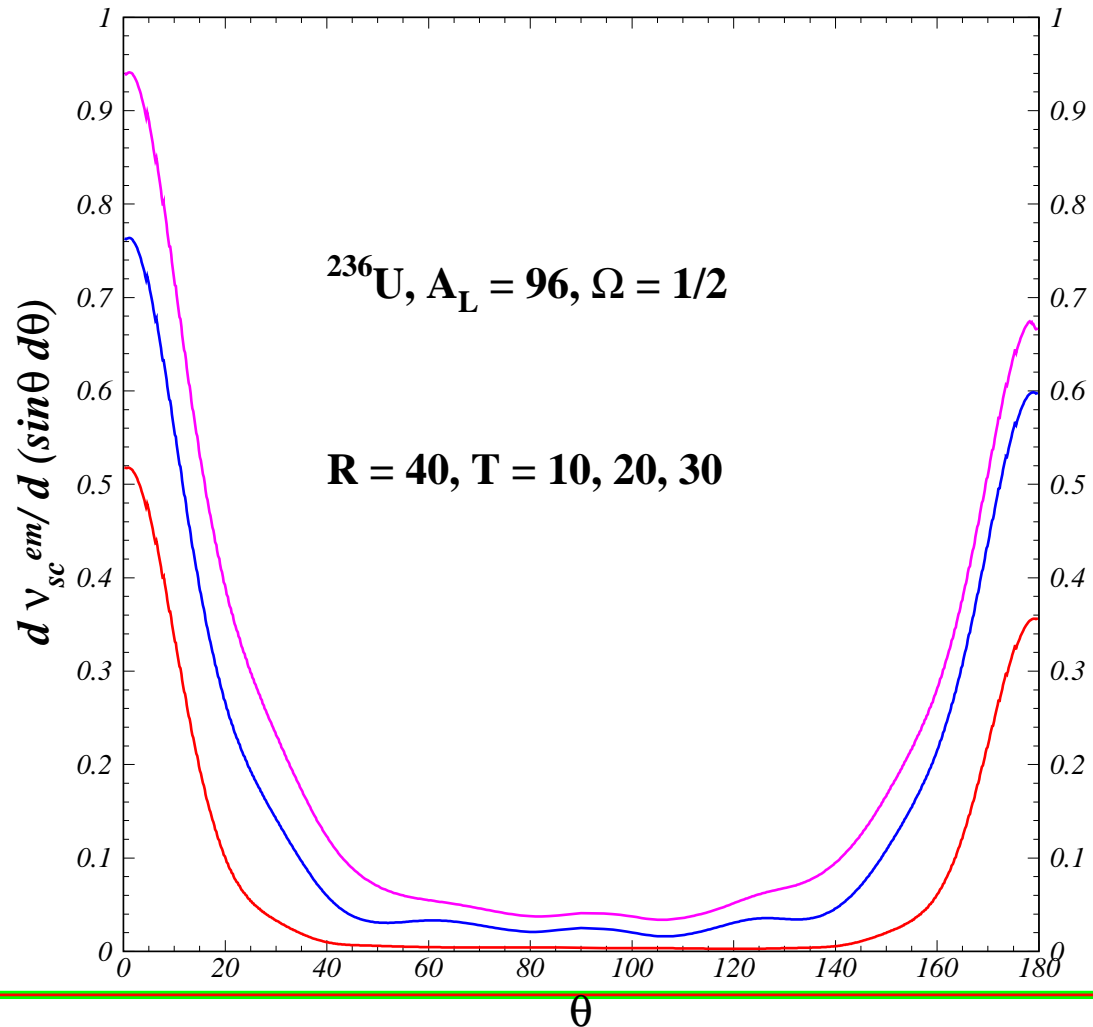
The time evolution of the angular distribution for $A_L = 70$

the emission seems to saturate faster than at $A_L = 96$



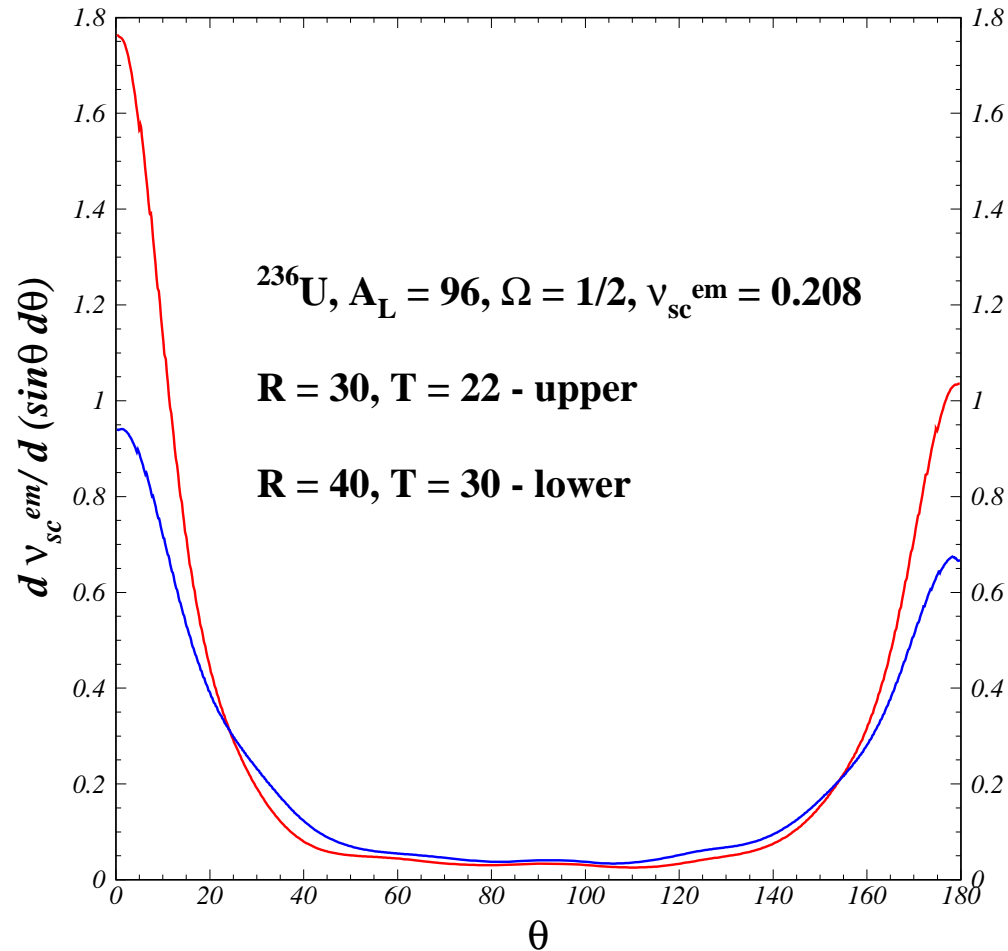
The time evolution of the ang distr for $A_L = 96$ at $R=40$ fm

L and H widths increase with increasing time T

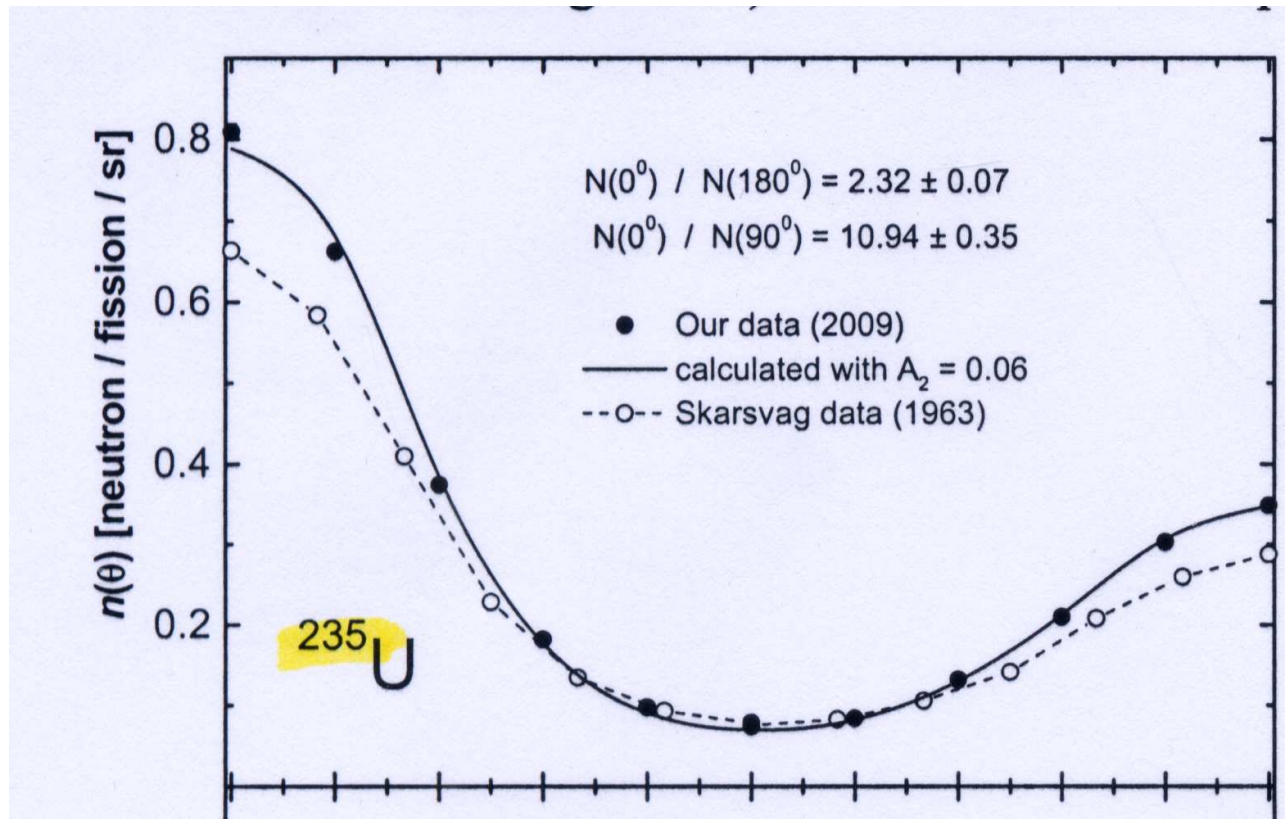


Comparison of the ang distr for $A_L = 96$ at $R=30$ and 40 fm

L and H widths increase with increasing radius R



Experimental distribution



A.S. Vorobyev et al., International seminar on interaction of neutrons with nuclei, Dubna, 2010. Note the resemblance with our calculations except the widths on both sides.

Scission neutron multiplicity - $\Omega = 1/2$

A_L		70		96		118	
		ν_{sc}	$\int S_{em}$	ν_{sc}	$\int S_{em}$	ν_{sc}	$\int S_{em}$
T	1	0.323	0.322	0.389	0.389	0.358	0.358
T		ν_{sc}^{em}	$\int S_{em}$	ν_{sc}^{em}	$\int S_{em}$	ν_{sc}^{em}	$\int S_{em}$
	10	0.087	0.236	0.096	0.293	0.099	0.259
	16	0.154	0.169	0.150	0.239	0.184	0.174
	20	0.186	0.137	0.188	0.201	0.223	0.136

The test relation $\nu_{sc}(1) = \nu_{sc}^{em}(T) + \int S_{em}(T)$ for $T > 1$ is well verified. Note that $\int S_{em}$ is calculated on the whole domain for $T = 1$, while for $T > 1$ it is evaluated only in the interior of the sphere of radius R .

Scission neutron multiplicity

A_L		70		96		118	
		ν_{sc}	ν_L/ν_H	ν_{sc}	ν_L/ν_H	ν_{sc}	ν_L/ν_H
T							
1		0.667	0.891	0.561	1.075	0.612	1.
T							
		ν_{sc}^{em}	ν_L/ν_H	ν_{sc}^{em}	ν_L/ν_H	ν_{sc}^{em}	ν_L/ν_H
10		0.109	1.759	0.118	1.424	0.121	1.
16		0.201	1.119	0.197	1.338	0.233	1.
20		0.247	1.056	0.258	1.348	0.283	1.

All the states corresponding to $\Omega = 1/2, \dots, 7/2$ have been taken into account. The ratio corresponds to two regions of the interval $(0, 180)$, the separation point being obtained in terms of the neck position. They represent neutrons which move left and right w.r. to a plane perpendicular to the neck.

Scission neutron multiplicity

A_L		70		96		118	
		ν_{sc}	ν_L/ν_H	ν_{sc}	ν_L/ν_H	ν_{sc}	ν_L/ν_H
T	1	0.667	0.891	0.561	1.075	0.612	1.
T		ν_{sc}^{em}	ν_L/ν_H	ν_{sc}^{em}	ν_L/ν_H	ν_{sc}^{em}	ν_L/ν_H
	10	0.109	1.901	0.118	1.448	0.121	1.
	16	0.201	1.231	0.197	1.374	0.233	1.
	20	0.247	1.218	0.258	1.378	0.283	1.

The ratio corresponds to the regions: $\theta \in [0, 50]$ and $\theta \in [130, 180]$.

Final remarks - angular distribution

The **angular distribution** of the neutrons emitted at scission is **calculated** starting **with initial conditions given by a realistic scission model** that is dynamical, microscopic and quantum mechanical. It uses nuclear configurations at scission that are appropriate for the main fission mode in the $^{235}\text{U}(n_{th}, f)$ reaction. Although the neutrons are mainly released in the interfragment region, they do not move perpendicular to the fission axis but are drained into the fragments (more into the light one) and finally leave the fissioning system through its tips. They therefore move along the fission axis with an average velocity not too far from the velocity of the fully accelerated fragments. Curiously enough, the ratio ν_L/ν_H is close to the experimental value (1.41) averaged over all fragment pairs.

Final remarks - angular distribution

Unusual process : simultaneous partial emission of all neutrons present in a fissioning nucleus at scission.

Limitations: due to the complexity of the calculations we were not so far able to:

- 1) Use a larger numerical grid than: $\rho_{max} = z_{max} = 35 fm$; but TBC were implemented at the numerical boundary.
- 2) Propagate the wave packet of the unbound neutrons longer than: $4 \times 10^{-21} s$; however the majority of neutrons have left the sphere by then.

Approximations recently tested:

- 1) role of the imaginary potential
- 2) effect of the separation of the fission fragments.

None affects the width. The ratio ν_L/ν_H is very little influenced.